

Multiple dynamical resonances in a discrete neuronal model

Yu Jiang

Departamento de Física, Universidad Autónoma Metropolitana-Iztapalapa, Apartado Postal 55-534, 09340 México, Distrito Federal México

and Programa de Ingeniería Molecular, Instituto Mexicano del Petróleo, Lázaro Cárdenas 152 07730 México, Distrito Federal, México

(Received 15 December 2004; published 26 May 2005)

The conditions for the occurrence of different multiple resonances in an excitable neuron model are analyzed numerically. It is shown that the excitable system may display both stochastic and coherence resonance, in response to periodic stimuli in the presence of different intensities of additive and parametric noises. It is found that double coherence resonances may take place in the low-amplitude oscillation regimes, and coherence resonance may persist even in the weak oscillatory regimes for control parameters slightly larger than the Hopf bifurcation point, where the system is in the incipient stage of large-amplitude excitation regime.

DOI: 10.1103/PhysRevE.71.057103

PACS number(s): 02.50.Ey, 05.40.-a, 84.35.+i, 05.45.Xt

Noise-induced resonance behavior in bistable, excitable, and other nonlinear dynamical systems near their bifurcation points has attracted considerable attention in recent years [1–7]. In a recent experimental study [8] on the photosensitive Belousov-Zhabotinsky reaction system stochastic (SR) and coherence (CR) resonances are found to occur at different noise intensities for an excitable system driven by noise and a periodic signal. It is therefore interesting to investigate the conditions under which such kinds of double resonance (i.e., stochastic and coherence resonances happening at different noise intensities for the same dynamical system) may occur. Multiple resonance phenomena have also been observed in a numerical study on the CO+O₂ catalytic oxidation reaction system, subject to multiplicative noise [9]. The mechanisms underlying SR and CR in excitable systems are well understood now. SR occurs when the mean escape time to threshold and the period of external forcing match. For excitable systems the situation may be complicated by the existence of system intrinsic oscillation, induced by the presence of an optimal amount of noise [10]. The interplay of external forcing and the noise-induced oscillation exhibits typical periodic resonance features, characterized by the appearance of various phase-locking modes. On the other hand, CR takes place when the frequency of noise-induced oscillation coincides with that of the system intrinsic oscillation, related usually to the Hopf bifurcation. From the time-scale matching theory it seems quite intriguing that double resonances occur in an autonomous dynamical system. It is therefore important to investigate under what conditions those multiple resonances may be observed for it may involve the selective enhancement of internal and external signals.

In this paper we analyze the conditions under which multiple resonance may be observed for different noise intensities in the same excitable system, focusing our attention on the roles played by forcing frequency and system bifurcation parameters. To this end we use a two-dimensional discrete-time neuron model system introduced by Rulkov [11], which displays complex dynamical behaviors as many other continuous dynamical systems do:

$$x_{n+1} = a/(1+x^2) - y_n + A \sin(\omega n) + D\xi_n,$$

$$y_{n+1} = y_n - b(x_n + 1), \quad (1)$$

where a and b are parameters that determine the model's dynamical behavior. The iteration number n plays the role of a discrete-time index. The fast variable x stands for the neuron cell membrane voltage, and y models the slow variation of ion concentration near the neuron membrane. The amplitude and frequency of periodic stimulus are denoted by A and ω , respectively. ξ_n is the Gaussian white noise, and D represents the noise intensity. In the absence of external perturbations, for the time-scale parameter $b=0.001$, the model system undergoes a Hopf bifurcation at $a=2$, and shows periodic oscillation for $2 < a < 4$, chaotic bursting for $4 < a < 4.6$, etc. It has been shown that for parameter a near the Hopf bifurcation point $a_H=2.0$, the system (1) can display SR and CR [12]. In addition to the additive external perturbations as described in Eq. (1), we consider also the Rulkov mode under multiplicative noise and periodic forcing,

$$x_{n+1} = a_n/(1+x^2) - y_n, \\ y_{n+1} = y_n - b(x_n + 1), \quad (2)$$

where the control parameter a_n is described by

$$a_n = a + A \sin(\omega n) + D\xi_n. \quad (3)$$

For simplicity, we restrict the analysis to only additive or multiplicative external stochastic and periodic driving. The case in which the system is driven simultaneously by both additive and multiplicative perturbations will be presented elsewhere. To quantify the structure of spikes induced by external perturbations we use the coefficient of variation of the interspike intervals defined by

$$R = \sqrt{\text{Var}(t_s)} / \langle t_s \rangle \quad (4)$$

where $\langle t_s \rangle$ and $\text{Var}(t_s)$ are the mean and the variance of the interspike interval t_s . The regular spiking is characterized by the minimum of R , while irregular excitations correspond to R close to 1. For excitable systems, SR is identified by comparison of the average spiking frequency with the periodic forcing frequency, which occurs at relatively low noise intensity. CR corresponds to a balance between the interspike interval of noise-induced spiking and the period of the sys-

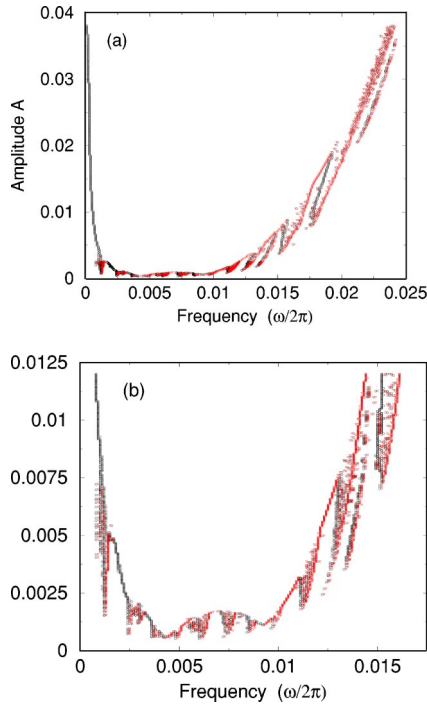


FIG. 1. (Color online) Plot of the amplitude-frequency threshold for Rulkov model with (a) additive periodic forcing, and (b) parametric or multiplicative periodic driving. The system control parameter is $a=1.99$. For a given forcing amplitude, the circles stand for the left boundary of the firing domains, and the triangles for the right one.

tem's intrinsic oscillation near the Hopf bifurcation point.

Before proceeding to the study of noise-induced cooperative oscillations, let us investigate first the dependence of the system's response to pure periodic stimuli on forcing frequency. Figure 1 shows the amplitude threshold for firing as a function of forcing frequency. For additive periodic forcing we find that there exist frequency-sensitive domains in the amplitude-frequency space where periodic forcing may induce excitation. For a given amplitude, there is an upper frequency limit $\omega_c(A)$ such that for $\omega > \omega_c(A)$ sinusoidal signals cannot trigger a spike. From Fig. 1(a) we see that the frequency-sensitive firing domain is bordered by a U-shaped curve with some complicated fine structures at the boundary areas. As will be shown later, the frequency-sensitive feature of an excitable system has an important impact on the resonance behavior. In Fig. 1(b) we plot the amplitude threshold curve for parametric driving (2). We found a similar U-shaped frequency-sensitive structure. Here even the low-frequency boundary displays riddling at small forcing amplitude. It seems that the insensitivity of the excitable Rulkov model to sinusoidal signals of high enough frequency persists even for very large forcing amplitude. In this kind of excitable system, the simple crossing of a bifurcation point in the system control parameter does not lead to spiking, and therefore the sinusoidal signals with their amplitude and frequency outside the frequency-sensitive regions should be taken as subthreshold. On the other hand, inside the excitation region, different non-self-oscillating regimes may be observed. For a given amplitude a typical scenario is formed by successive frequency intervals of phase-locking patterns 1:2,

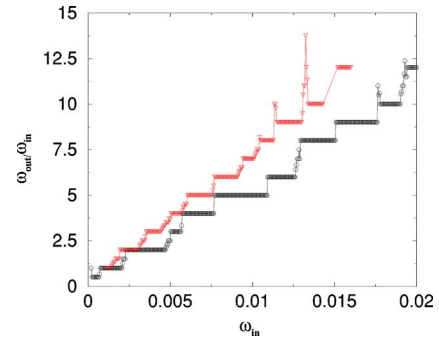


FIG. 2. (Color online) Typical devil's staircase structure of the phase-locking patterns for periodically driven Rulkov model in the firing regimes, for additive forcing at $A=0.03$ (circles) and parametric driving at $A=0.016$ (triangles), respectively. ω_{in} represents the frequency of the input signal, and ω_{out} is that for the system output. Here the output frequency is calculated from the mean interspike interval, i.e., $\omega_{out}=1/\langle t_s \rangle$.

1:3, 1:4, etc., with possible irrational phase-locking modes in between, revealing the structure of the devil's staircase. Since the system is in the firing regime, a stimulus pulse may induce several spikes, depending on the forcing amplitude. So one finds that the output frequency increases with the input one. Figure 2 shows the ratio of the output frequency and the forcing frequency as a function of the latter for additive and multiplicative (parametric) periodic driving. As shown in [13] the phase locking, period doubling, and possible chaotic phenomena in externally driven excitable systems can be attributed to the competition between the system intrinsic frequency and the external one, similar to the well-known phase-locking structure of driven self-oscillator and circle maps. It is interesting to note that in the case of multiplicative forcing, even for suprathreshold sinusoidal stimuli with $a_0+A > 2.0$, there still exist frequency-sensitive excitation domains in the amplitude-frequency plane. The inactivity of the excitable Rulkov model for certain high-frequency signals is related to the duration time for a pulse to stay over the excitation threshold. This observation is consistent with our findings for the excitable FitzHugh-Nagumo neuron model, but is in contrast with other excitable systems such as the Hindmarsh-Rose neuron model [14] and the photosensitive Belousov-Zhabotinsky reaction system, where suprathreshold periodic signals of arbitrary frequency produce excitation. It should be stressed that the amplitude threshold phase diagrams are the basis for our understanding of the effects of forcing frequency on the resonance behavior of the excitable Rulkov model system.

(1) *Dependence of SR on forcing frequency.* SR occurs when a match between the period of external forcing and the first-passage time is achieved. If the periodic stimuli are weak, SR is expected to be observed for low noise strength. In this case CR is the dominant resonance pattern at intermediate and large noise intensity. It is expected that as the forcing frequency increases, the optimal noise intensity for SR shifts toward larger noise strength accordingly. Figure 3(a) plots the coefficient of variation $R(D)$ as a function of the noise intensity D for several forcing frequencies for $a = 1.99$ and $A=0.025$ for additive stochastic and periodic forc-

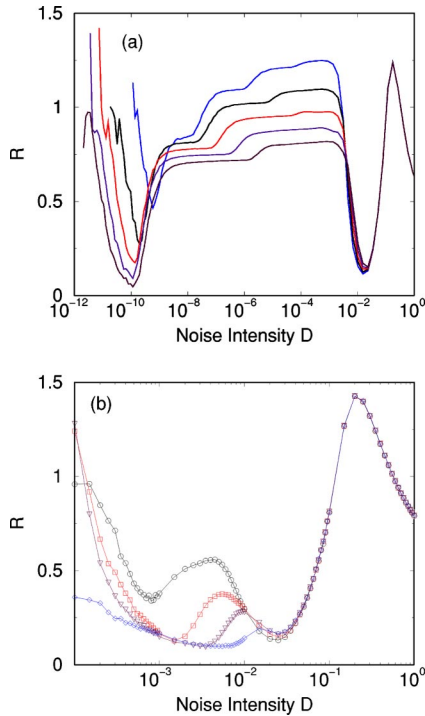


FIG. 3. (Color online) Stochastic and coherence resonance in the Rulkov model. The coefficient of variation R is plotted as a function of the noise intensity for (a) additive external perturbations with forcing amplitude $A=0.025$ and forcing frequency $\omega=2\pi \times 10^{-4}$, $2.5\pi \times 10^{-4}$, $3\pi \times 10^{-4}$, $3.5\pi \times 10^{-4}$, and $4\pi \times 10^{-4}$ (from top to bottom), and (b) multiplicative modulations at $A=0.0099$ and $\omega=4\pi \times 10^{-4}$ (circles), $8\pi \times 10^{-4}$ (squares), $1.2\pi \times 10^{-3}$ (triangles), and $1.6\pi \times 10^{-3}$ (diamonds).

ing. It is shown clearly that the forcing frequency has a drastic impact on SR, but little effect on CR. As the forcing frequency is increased and is approaching the firing-nonfiring boundary from below in the amplitude-frequency space, the SR becomes stronger and disappears once the frequency is in the firing region. At first glance, it seems to be rather puzzling that the location of SR shifts to lower values of noise intensity D , instead of to larger values as required by the match between the first-passage time induced by noise and the intrinsic oscillation period of the system. Nevertheless, if we take into account the fact that the system approaches the firing domain as ω increases, it is obvious that less noise is required when the system is closer to the firing threshold. Another intriguing phenomenon is the noise-induced phase-locking patterns as illustrated by the staircase structure of the resonance curve for the noise intensity between $D=10^{-10}$ and 10^{-2} . For instance, at forcing frequency $\omega=4\pi \times 10^{-4}$, we find that $\omega_{\text{out}}:\omega_{\text{in}}=2:1$ for $10^{-8} < D < 10^{-6}$, and $\omega_{\text{out}}:\omega_{\text{in}}=3:1$ for $10^{-5} < D < 10^{-3}$, approximately. The optimal noise intensity for CR, on the other hand, remains almost unchanged. As the forcing frequency is further increased, the system enters the frequency-sensitive firing regimes, where weak noise can destroy the regular spiking, and generate a kind of bursting mode. It is remarkable that in the firing regime we still observe CR, for the system's response at the intermediate through large noise intensity is completely dominated by the noise. In Fig. 3(b) we

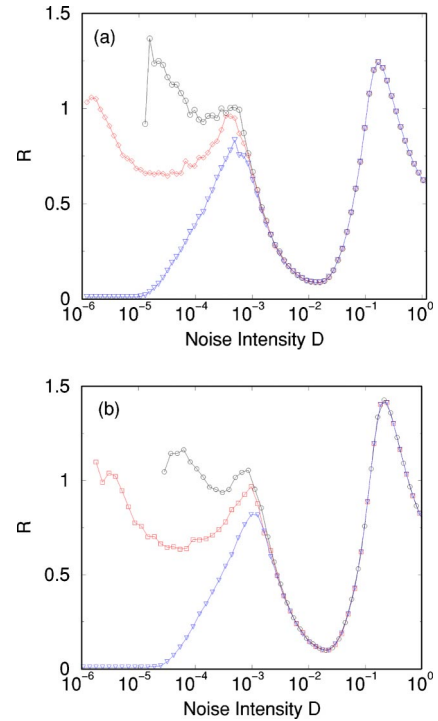


FIG. 4. (Color online) Double coherence resonance observed in Rulkov neuron model under (a) additive and (b) multiplicative noise driving, for $a=1.9989$ (circles), 1.999 (diamonds), and 1.9992 (triangles).

plot R as a function of the noise intensity D for multiplicative or parametric noise and periodic perturbations. Here we see that the double-valley resonance curve that appears at low frequency is replaced by a single-valley one as the frequency increases. While the position of CR remains unchanged, the location of SR shifts to larger noise intensity, which is consistent with the requirement of a time-scale match between the first-passage time induced by noise and the period of external forcing, but in sharp contrast with the case of additive forcing.

(2) *Double CR in small-amplitude oscillation regimes.* In the context of CR, the condition for the occurrence of multiple resonances at different noise intensities may be attributed to the existence of multifrequency oscillations. Figure 4 shows the double CR for the Rulkov neuron model in the absence of external periodic forcing, i.e., $A=0$. We find that the first CR occurs only within a narrow range of the control parameter a , and its coherence effect is much weaker than that of the second (the standard) CR. It is seen that the optimal noise intensity for the occurrence of CR, D_{CR} , decreases with increasing a . The mechanism of the leftmost resonance valley may be understood as follows. For $1.998 < a < 1.999$ the Rulkov model system exhibits low-amplitude oscillation, and its frequency decreases with increasing a . So it is easy to understand why the optimal noise intensity at which the noise-induced oscillation matches the intrinsic low-amplitude oscillation moves to smaller noise strength as a increases. Interestingly we find this phenomenon for Rulkov model with additive and multiplicative noise, as well. We notice that for the $\text{CO}+\text{O}_2$ catalytic oxidation reaction system discussed in [9], there exists also a low-amplitude oscil-

lation range, with its amplitude decreasing with the distance of the control parameter to the bifurcation point. Since the peak height of the resonant oscillation is used as a measure in that work, it is difficult to infer the mechanism behind the very intriguing double-CR phenomenon, where the leftmost CR appears to be stronger than the rightmost one. In our case, the intrinsic frequency of small-amplitude oscillation is a function of the bifurcation parameter a . Weak noise cannot perturb the system's dynamics, and strong enough noise will drive the system into oscillatory regimes. Thus, there exists an optimal noise intensity that produces this weak-noise CR.

(3) *CR in oscillatory regimes.* For the system control parameter $a > 1.999$, the Rulkov model displays spikes, or large-amplitude oscillations. As already illustrated in Fig. 4, CR may be observed in this parameter regimes. In Fig. 5 we plot R against the noise intensity D , for a slightly larger than 2. This happens because the oscillation in this parameter range is very weak, and is strongly affected by external perturbations. Interestingly this internal SR [15] occurs at the same noise intensity as the CR when $a < 2$. As a increases further into the strong-oscillation regime, the peak related to noise-induced irregularity disappears. An inspection of the time evolution of the system variables for $a=2.0$ shows that noise produces irregular suppression of firing at $D=0.001$, and more regular firing is recovered at $D_{CR}=0.02$, approximately.

In conclusion, in this work we present a detailed numerical analysis of multiple-resonance behaviors in the Rulkov neuron model, which proves to be an efficient vehicle for instigation of the dynamical response of more complex excitable neuron model systems to various stochastic and periodic stimuli. We studied the conditions for which the system can respond to different noise through SR and CR. We explained the mechanism for the appearance of double CR as the existence of a continuously changed oscillation frequency as a function of the control parameter a after the Hopf bifurcation. The CR in the firing regimes and CR in the oscillatory states are attributed to the weak, initial stage of the oscillation, which turns out to be very vulnerable to external noise. Another interesting phenomenon exhibited by the Rulkov neuron model is anticoherence or incoherence maximization, characterized by $R > 1$ [16,17]. The anticoher-

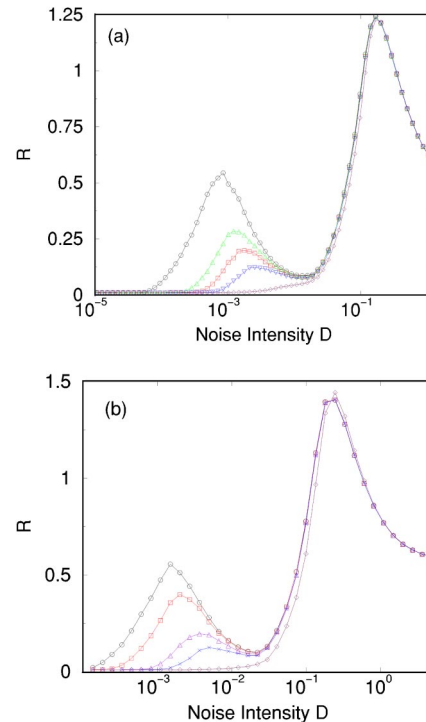


FIG. 5. (Color online) Coherence resonance in the oscillatory regimes for Rulkov model subject to (a) additive and (b) multiplicative stochastic and periodic perturbations. The system control parameter $a=2.0, 2.0025, 2.005, 2.01, \text{ and } 2.05$ in (a), and $a=2.0, 2.001, 2.005, 2.01, \text{ and } 2.1$ in (b) (from top to bottom).

ence resonance may occur for different physical situations. For the FitzHugh-Nagumo model it occurs at low noise in the presence of damped subthreshold oscillations [17], while for the leaky integrate-and-fire model, the incoherence maximization appears in the noise-activated firing regime for sufficiently small values of the absolute refractory period [16]. From the time evolution of the system variable, the maxima of R for the Rulkov model seem to be related to the transition from random bursting and complete irregular spiking.

[1] L. Gammaitoni, P. Hanggi, P. Jung, and F. Marchesoni, *Rev. Mod. Phys.* **70**, 223 (1998).
 [2] Hu Gang, T. Dizinger, C. Z. Ning, and H. Haken, *Phys. Rev. Lett.* **71**, 807 (1993).
 [3] D. Sigeti and W. Horsthemke, *J. Stat. Phys.* **54**, 1217 (1989).
 [4] A. S. Pikovski and J. Kurths, *Phys. Rev. Lett.* **78**, 775 (1997).
 [5] S. Ripoll Massanes and C. J. Perez Vicente, *Phys. Rev. E* **59**, 4490 (1999).
 [6] A. Neiman, P. I. Saporin, and L. Stone, *Phys. Rev. E* **56**, 270 (1997).
 [7] B. Lindner, J. Garcia-Ojalvo, A. Neiman, and L. Schumansky-Geier, *Phys. Rep.* **392**, 321 (2004).
 [8] K. Miyakawa, T. Tanaka, and H. Isikawa, *Phys. Rev. E* **67**, 066206 (2003).
 [9] Z. Hou, L. Yang, and H. Xin, *J. Chem. Phys.* **111**, 1592

(1999).
 [10] A. Longtin and D. R. Chialvo, *Phys. Rev. Lett.* **81**, 4012 (1998).
 [11] N. F. Rulkov, *Phys. Rev. Lett.* **86**, 183 (2001).
 [12] R. C. Hilborn, *Am. J. Phys.* **72**, 528 (2004).
 [13] M. Feingold, D. L. Gonzalez, O. Piro, and H. Viturro, *Phys. Rev. A* **37**, 4060 (1988).
 [14] W. Wang, Y. Wang, and Z. D. Wang, *Phys. Rev. E* **57**, R2527 (1998).
 [15] Q. S. Li and R. Zhu, *J. Chem. Phys.* **115**, 6590 (2001).
 [16] B. Lindner and L. Shimansky-Geier, *Phys. Rev. E* **66**, 031916 (2002).
 [17] A. M. Lacasta, F. Sagues, and J. M. Sancho, *Phys. Rev. E* **66**, 045105(R) (2002).